Applied Mathematics and Computation 252 (2015) 263–272

Contents lists available at ScienceDirect

Applied Mathematics and Computation

journal homepage: www.elsevier.com/locate/amc

Asymptotic number of $\mathbb{Z}^3\Delta$ cells covering $\mathcal{C}^{(1)}$ surface on uniform grid and complexity of recursive-partitioning simulation of septal tissue regions

Marko D. Petković [a,*], Predrag R. Bakic [b], Andrew D.A. Maidment [b], David Pokrajac [c]

[a] University of Niš, Faculty of Science and Mathematics, Višegradska 33, 18000 Niš, Serbia
[b] Department of Radiology, University of Pennsylvania, Philadelphia, PA 19104, USA
[c] Computer and Information Sciences Department, Applied Mathematics Research Center, CREOSA Center, Delaware State University, Dover, DE 19901, USA

ARTICLE INFO

Keywords:
Octree
$\mathcal{C}^{(1)}$-surface
Recursive partitioning
Medical image simulation

ABSTRACT

The exact asymptotic computational complexity for a problem of indexing cells on a uniform grid intersecting with a union of $\mathcal{C}^{(1)}$ surfaces has been proven. The computational complexity of the recursive partition indexing algorithm, utilized for simulation of septated tissues, is derived and the algorithm is demonstrated as being asymptotically optimal.

1. Introduction

Octrees (e.g., [1–3]), a 3*D* spatial indexing technique, have successfully been used in various applications in imaging and computer graphics. For example, octrees are utilized for efficient data representation in fast interactive rendering of isosurfaces [4], rendering of medical data [5,6], 3*D* surface-based thinning algorithms [7] and compression of complex isosurfaces [8]. Recent parallel applications of octrees include [9,10].

The need for preclinical validation and optimization of medical imaging systems or image analysis methods has recently led to the development of a recursive partitioning based simulation technique (e.g., [10–15]). In this technique, an organ of interest is specified using a system of scalar fields in 3*D* space. Various anatomic constituents of the organ (compartments, septal regions separating compartments, skin, etc.) are modeled by indexing voxels or groups of voxels using octrees. The recursive partitioning stops when the linear dimension of a cubic subdomain is equal to the prespecified size or when the cubic subdomain contains material of a single type.

The use of octree-based recursive partitioning in breasts simulation has led to a number of significant accomplishments. The GPU implementation allows for near real-time modeling of the breast; software phantoms are generated at a rate of 7 breasts/minute using a voxel resolution of 50 micrometers [10]. In addition, the method makes it possible to simulate the breast, in whole or in part, at the cellular level [11]. Use of the accelerated simulation at high spatial-resolution provides an avenue for realistically modeling of breast microstructures [16,17]. These accomplishments enable the simulation of clinical trials on a per patient basis. These virtual clinical trials have become a feasible option for conducting preclinical testing of novel breast imaging systems [18]. The successes arising from simulation of the breast anatomy support the extension of octree-based recursive partitioning to the simulation of other septated tissues (e.g., cortical bone, lung parenchyma), as well

* Corresponding author.
E-mail addresses: dexterofnis@gmail.com (M.D. Petković), Predrag.Bakic@uphs.upenn.edu (P.R. Bakic), Andrew.Maidment@uphs.upenn.edu (A.D.A. Maidment), dpokrajac@desu.edu (D. Pokrajac).

http://dx.doi.org/10.1016/j.amc.2014.11.111
0096-3003/

Notation

B	lattice (coordinate) box
K	number of partition functions
L	octree depth
ϕ_i	functions that partition box $B^{(0)}$ (shape functions)
$B^{(0)}$	initial cubic box
$B^{(l)}$	set of initial cubic box subdivisions with side length $\Delta^{(l)}$
B_{kl}	cell of a 2D lattice; projection of B onto xy plane
$\mathcal{B}^{(l)}$	set of all boxes $B^{(l)}$
$\dim_b(X)$	box-counting dimension of bounded set X
η	node of the octree
$\eta.\Phi$	set of shape functions associated with node η
$\eta.B$	cubic subdomain associated with node η
$\Delta^{(0)}$	side length of $B^{(0)}$
$\Delta^{(l)}$	$\Delta^{(0)}/2^l$ – side length of $B^{(l)}$
$\Phi^{(0)}$	set of shape functions
$\mathbb{Z}^3\Delta, \mathbb{Z}^2\Delta$	3D and 2D coordinate lattice with unit size Δ
p_L	total number of octree nodes up to level L
u_l	number of nodes at level l with subvolumes intersecting $\mathcal{S}$
v_l	number of nodes at level l of an octree
$C_k, k = 1, 2, \ldots, K$	subdomains of $B^{(0)}$, compartments
$N_X(\Delta), N_{\mathcal{S}}(\Delta), N_\gamma(\Delta)$	number of boxes from $\mathbb{Z}^3\Delta$ intersecting with a bounded set $X, \mathcal{S}, \gamma$
$P(\mathcal{S})$	$N_{\mathcal{S}}(\Delta)\Delta^2$
$\mathcal{C}^{(1)}(X)$	set of all continuously differentiable functions, defined on the set X
$\mu(X)$	lebesgue measure of the set X
$\overline{F}_{k,l}$	normalized maximal value of function f on $\mathcal{S}_{xy} \cap B_{kl}$
$\underline{F}_{k,l}$	normalized minimal value of function f on $S_{xy} \cap B_{kl}$
R	union of rectangles R_i
R_i	rectangle on $\mathcal{S}_{xy}$
$\mathcal{S}$	union of all boundaries $\mathcal{S}_{ij}$; a surface
$\mathcal{S}_{ij}$	boundary of subdomains C_i and C_j
$\mathcal{S}_{xy}, \mathcal{S}_{xz}, \mathcal{S}_{yz}$	projections of surface S on coordinate planes; $\mathcal{S}_{xy}$ also denotes rectangle on plane xy
$\mathcal{S}_R$	surface induced by R
$M_{\mathcal{S}}$	$\max_{(x,y)\in\mathcal{S}_{xy}} \frac{\partial f}{\partial x}(x,y) + \max_{(x,y)\in\mathcal{S}_{xy}} \frac{\partial f}{\partial y}(x,y) + 2$
γ	finite union of $\mathcal{C}^{(1)}$ curves; A set with box-counting dimension <2
$\delta\mathcal{S}, \delta X$	boundaries of $\mathcal{S}, X$

as various porous materials [19]. To support the widespread application of this method and fully exploit the benefits, especially for multi-scale simulation tasks, a better understanding of its theoretical computational complexity is needed. This is the motivation for our work.

Note that the problem considered in [11] can be reduced ultimately to the problem of indexing voxels intersecting with a union of 3D $\mathcal{C}^{(1)}$ surfaces. The computational complexity of a recursive partitioning algorithm for approximation of 3D implicit *polynomial* surfaces was discussed in [20]. In that paper, using a concept of ϵ-entropy (the minimal number of closed balls of radius ϵ covering the surface), an upper bound for the algorithm complexity was proven. However, the problem of the lower bound of the problem, as well as the computational complexity of the similar, but not equivalent, problem discussed in [11] has remained open. Observe that experimental results [10,11] have indicated that the computational complexity of the recursive algorithm proposed to solve the problem is quadratic w.r.t. the reciprocal linear dimension of a voxel. This has led to the hypothesis that the asymptotic complexity of the algorithm is quadratic. Further, we wanted to examine the hypothesis that the algorithm is computationally optimal, which warrants determination of the lower bound of the complexity.

In this paper, we formally restate the considered problem and the recursive partitioning algorithm in Section 2. In Section 3, we demonstrate a quadratic computational complexity of the indexing algorithm. In addition, we demonstrate that the influence of the overhead introduced by recursive partitioning of the domain does not increase the asymptotic complexity of the algorithm. In Section 4, we formally prove the asymptotic number of uniform 3D cubic cells covering a finite union of $\mathcal{C}^{(1)}$ surfaces, which is the main result in Section 3.

2. Recursive partitioning indexing algorithm

Consider a cubic box $B^{(0)} \subset \mathbb{R}^3$ and functions $\phi_i \in \mathcal{C}^{(1)}(B^{(0)}), i = 1, 2, \ldots, K$ (hereafter referred to as *shape functions*). Define

$$\mathrm{md}(\mathbf{x}) = \min_{1\leqslant j\leqslant K}\phi_j(\mathbf{x}).$$

The shape functions partition $B^{(0)}$ into K subdomains $C_1, C_2, \ldots, C_K$ defined by

$$C_k = \left\{\mathbf{x} \in B^{(0)} \mid \phi_k(\mathbf{x}) = \mathrm{md}(\mathbf{x})\right\}, \quad k = 1, 2, \ldots, K.$$

In other words, the set C_k is set of all points $\mathbf{x} \in B^{(0)}$ such that $\phi_k(\mathbf{x})$ is smallest among all values $\phi_j(\mathbf{x})$ for $j = 1, 2, \ldots, K$. These subdomains C_k are hereafter referred to as *compartments*. Note that compartments C_k provide a suitable generalization of Voronoi diagrams. Denote by $\mathcal{S}_{i,j}$ the common boundary of C_i and C_j $(1 \leqslant i < j \leqslant K)$. Note that $\mathcal{S}_{i,j}$ may be an empty set if C_i and C_j do not have a common boundary. Furthermore, denote by $\mathcal{S}$ the union of all boundaries, i.e.,

$$\mathcal{S} = \bigcup_{1\leqslant i<j\leqslant K} \mathcal{S}_{i,j} \tag{1}$$

It is obvious that all $\mathcal{S}_{i,j}$ are $\mathcal{C}^{(1)}$ surfaces implying that $\mathcal{S}$ is a piecewise $\mathcal{C}^{(1)}$ surface. We consider the following problem of indexing the boundaries of the compartments.

Assume that each side of the initial box $B^{(0)}$ with side length $\Delta^{(0)}$, is divided into a total 2^l equal parts. The entire box is therefore divided into a total of 2^{3l} subboxes of unit size $\Delta^{(l)} = \Delta^{(0)}/2^l$. Denote the set of all such subboxes by $\mathcal{B}^{(l)}$.

Problem 1 (***BoxApprox***). For a fixed $L \in \mathbb{N}$, find all subboxes $B \in \mathcal{B}^{(L)}$ of $B^{(0)}$ having non-empty intersection with $\mathcal{S}$. In other words, find all subboxes $B \in \mathcal{B}^{(L)}$ having non-empty intersection with at least two compartments C_k.

Note that $\mathcal{S}$ is a bounded surface. By an appropriate shift of the coordinate system, we obtain that all subboxes $B \in \mathcal{B}^{(L)}$ are coordinate boxes of a $\mathbb{Z}^3\Delta^{(L)}$ coordinate lattice (i.e., a coordinate lattice with a unit size $\Delta^{(L)}$). Hence, we need to determine the set of all coordinate boxes B of $\mathbb{Z}^3\Delta^{(L)}$ having non-empty intersection with $\mathcal{S}$.

A recursive partitioning algorithm to resolve this problem, which in addition indexes compartments, has been proposed [11]. The algorithm maintains an octree corresponding to $B^{(0)}$. Each node η at the level l of the octree is associated with a cubic subdomain $\eta.B \in \mathcal{B}^{(l)}$ of interest. Also, for each node the set $\eta.\Phi$ of shape functions is kept such that

$$\eta.\Phi = \{\phi_i \mid \phi_i(\mathbf{x}) = \mathrm{md}(\mathbf{x}), \text{ for some } \mathbf{x} \in \eta.B\}.$$

in a breadth-first fashion [21]. Nodes at each level of the tree are successively examined; if $\eta.B$ does not intersect $\mathcal{S}$ (i.e., $\eta.\Phi$ is a one element set) the node is not further split. Otherwise, the node is split into eight nodes $\eta_1, \eta_2, \ldots, \eta_8$ of the subsequent tree level $l+1$ and the corresponding values $\eta_k.B$ and $\eta_k.\Phi$ are determined. The recursive partitioning procedure continues until the tree depth L is reached. The algorithm from [11] can be conceptualized using the pseudocode notation, shown in Algorithm 2.1. Note that the function *SplitVolume* extracts a kth subvolume $\eta_k.B$ from a given volume $\eta.B$. The function *RefineShapeFunctions* determine which shape functions $\eta_k.\Phi$ are associated to a subvolume $\eta_k.B$, based on the shape functions $\eta.\Phi$ associated to a node η.

Algorithm 2.1. RecursivePartitionIndexing($B^{(0)}; \Phi^{(0)}; L; K$)

Require: Root volume $B^{(0)}$, shape functions $\Phi^{(0)} = \{\phi_1(\mathbf{x}), \phi_2(\mathbf{x}), \ldots, \phi_K(\mathbf{x})\}$; and the depth L of the octree
Root.$B := B^{(0)}$
Root.$\Phi := \Phi^{(0)}$
for level l :=0 to *L-1* **do**
  for each octree node η at level l
    if $|\eta.\Phi| > 1$ **then**
      Split the node η into identical-sized, level $l+1$ subnodes $\eta_k, k = 1, \ldots, 8$
      for $k := 1$ to 8 **do**
        $\eta_k.B := \mathit{SplitVolume}(\eta.B, k)$
        $\eta_k.\Phi := \mathit{RefineShapeFunctions}(\eta_k.B, \eta.\Phi)$
      end for
    end if
  end for
end for
for each leaf node η in the tree **do**
  return $\eta.B, \eta.\Phi$
end for

3. Computational complexity

In this section, we provide the computational complexity of Problem 1 and Algorithm 2.1. Denote by $N_X(\Delta)$ the number of boxes from lattice $\mathbb{Z}^3\Delta$ (i.e., a coordinate lattice with unit size Δ) having non-empty intersection with bounded set $X \subset \mathbb{R}^3$.

3.1. Asymptotic complexity of problem 1

The computational complexity of Problem 1 is determined by the number $N_{\mathcal{S}}(\Delta^{(L)})$ of cubes $B^{(L)} \in \mathcal{B}^{(L)}$. Recall that $\Delta^{(L)} = \Delta^{(0)}/2^L$ where $\Delta^{(0)}$ is the size of initial bounding box $B^{(0)}$.

The following theorem, utilized in the rest of this Section, is proven in Section 4.

Theorem 3.1. *Assume that $\mathcal{S} \subset \mathbb{R}^3$ is a bounded, piecewise $\mathcal{C}^{(1)}$ surface. Then $N_{\mathcal{S}}(\Delta)\Delta^2 \to const$ when $\Delta \to 0$.*

The Theorem 3.2 below directly gives the asymptotic computational complexity of the Problem 1.

Theorem 3.2. *The asymptotic computational complexity of Problem 1 is $\Theta(2^{2L})$. In other words, the number $N_{\mathcal{S}}(\Delta^{(L)})$ of all subboxes $B^{(L)} \in \mathcal{B}^{(L)}$ having non-empty intersection with $\mathcal{S}$ is asymptotically $\Theta(2^{2L})$.*

Proof. It is easy to see that $\mathcal{S}$ defined by (1) is piecewise $\mathcal{C}^{(1)}$ surface, since all $\phi_i(\mathbf{x}), i = 1, 2, \ldots, K$ are $\mathcal{C}^{(1)}$ functions. The statement of the theorem now follows from Theorem 3.1. □

3.2. Asymptotic complexity of recursive partitioning algorithm

Denote by v_l, the number of nodes at level l of the tree. Let u_l denote the number of nodes intersecting the surface $\mathcal{S}$ at level l of the tree. Denote by p_L, the total number of nodes of the octree on levels $1, 2, \ldots, L$. As demonstrated in [11], function *SplitVolume* has $\mathcal{O}(1)$ complexity. Also, function *RefineShapeFunctions* has $\mathcal{O}(K)$ complexity. Hence, the computational complexity of the Algorithm 2.1 is $\mathcal{O}(p_L)$.

The number of nodes u_l in the level l of the tree containing the compartment boundaries is equal to the number $N_{\mathcal{S}}(\Delta^{(l)})$ of cubes with linear dimension $\Delta^{(l)} = \Delta^{(0)}/2^l$ containing the boundaries. Fig. 1 visualizes the octree we are considering. Black nodes depict the tree nodes containing compartment boundaries (intersecting the surface $\mathcal{S}$). Gray nodes contain only compartments. Note that u_l is the number of black, while v_l is the number of both black and gray nodes at level l.

Our main tools in the proof of an asymtotic formula for p_L are Corollary 3.1 (following directly from Theorem 3.1) and Lemma 3.1.

Corollary 3.1. *There exists a constant C and a sequence $\omega_l \to 0$ $(l \to +\infty)$ such that $u_l/4^l = C + \omega_l$.*

Lemma 3.1. *Assume that δ_l is any sequence such that $\delta_l \to 0$ when $l \to +\infty$. Denote by*

$$\gamma_L = \frac{\delta_{L-1}}{4} + \frac{\delta_{L-2}}{4^2} + \cdots + \frac{\delta_0}{4^L}.$$

Then $\gamma_L \to 0$ when $L \to +\infty$.

Proof. Fix $\epsilon > 0$ and denote by L' the number such that $|\delta_l| < \epsilon$ for every $l > L'$. For each $L > L'$ holds

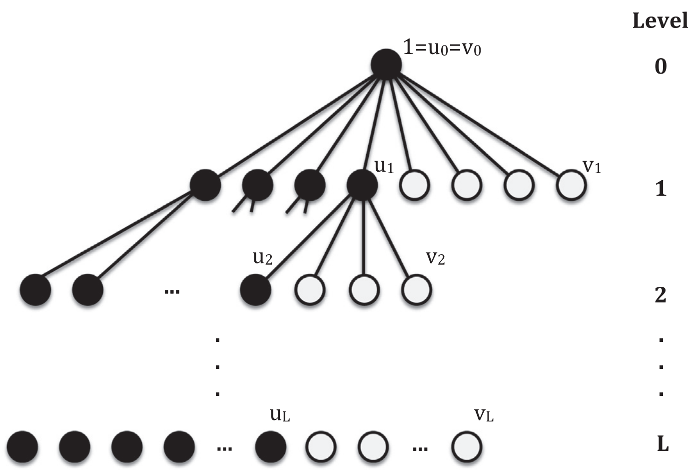

Fig. 1. Visualization of the octree. Black nodes depict the tree nodes containing compartment boundaries (intersecting the surface $\mathcal{S}$). Gray nodes contain only compartments. The number of black nodes at level l and the total number of nodes at the level l are denoted with u_l and v_l, respectively.

$$\begin{aligned}|\gamma_L| &\leqslant \left|\tfrac{\delta_{L-1}}{4}+\tfrac{\delta_{L-2}}{4^2}+\cdots+\tfrac{\delta_{L'}}{4^{L-L'}}\right|+\left|\tfrac{\delta_{L'}}{4^{L-L'}}+\tfrac{\delta_{L'-1}}{4^{L-LL'+1}}+\cdots+\tfrac{\delta_0}{4^L}\right| \\ &\leqslant \epsilon\left(\tfrac{1}{4}+\tfrac{1}{4^2}+\cdots+\tfrac{1}{4^{L-L'+1}}\right)+\tfrac{1}{4^{L-L'}}\left|\delta_{L'}+\tfrac{\delta_{L'-1}}{4}+\cdots+\tfrac{\delta_0}{4^{L'}}\right| \\ &= \epsilon\tfrac{1-4^{-(L-L'+1)}}{3}+4^{-(L-L')}h(L')\end{aligned}$$

where

$$h(L') = \left|\sum_{l=0}^{L'} 4^{-l}\delta_{L'-l}\right|$$

does not depend on L. It is possible to choose sufficiently large L, so that $4^{-(L-L')}h(L') < 2\epsilon/3$ and subsequently $|\gamma_L| < \epsilon$. This completes the proof of lemma. □

However, p_L is directly proportional to the computation complexity of Algorithm 2.1 and equal to

$$p_L = v_0 + v_1 + \cdots + v_L = 1 + 8(u_0 + u_1 + \cdots + u_{L-1}).$$

According to Corollary 3.1:

$$p_L = 1 + 8C(4^0 + 4^1 + \cdots + 4^{L-1}) + 8(\omega_0 + \omega_1 4^1 + \cdots + \omega_{L-1}4^{L-1})$$

and hence

$$\frac{p_L}{4^L} = 4^{-L} + 8C\frac{1-4^{-L}}{3} + \frac{\omega_{L-1}}{4} + \frac{\omega_{L-2}}{4^2} + \cdots + \frac{\omega_0}{4^{L-1}}.$$

According to Lemma 3.1 we get

$$\lim_{L\to+\infty}\left|\frac{p_L}{4^L} - 8C\frac{1-4^{-L}}{3}\right| = 0$$

implying that

$$\lim_{L\to+\infty}\frac{p_L}{4^L} = \frac{8C}{3} \quad\Rightarrow\quad p_L = \Theta(4^L). \tag{2}$$

According to this subsection (especially (2)), the following theorem holds:

Theorem 3.3. *The computational complexity of Algorithm 2.1 is* $\Theta(4^L)$.

4. Asymptotic number of Z^3 cells covering a piecewise $\mathcal{C}^{(1)}$ surface

Formal proof of Theorem 3.1 is provided stepwise in this section. From this point forward, let $\mathcal{S}$ represent an arbitrary (piecewise) $\mathcal{C}^{(1)}$ surface and $\Delta > 0$ is a real number.

4.1. Statement of the problem

Let $\mathcal{S} \subset \mathbb{R}^3$ be the surface and denote by $\mathcal{S}_{xy}, \mathcal{S}_{yz}$ and $\mathcal{S}_{xz}$ its projections to the xy, yz and xz coordinate planes. Assume that $\mathcal{S}$ can be represented as the graph of the function defined on $\mathcal{S}_{xy}$, i.e.,

$$\mathcal{S} = \{(x, y, f(x, y)) \mid (x, y) \in \mathcal{S}_{xy}\} \tag{3}$$

where $f : \mathcal{S}_{xy} \to \mathbb{R}$ is $\mathcal{C}^{(1)}$ function and $\mathcal{S}_{xy}$ is compact. Also assume that the boundary of $\mathcal{S}$ is a finite length curve.

Recall that, by $N_X(\Delta)$ we denote the number of boxes from lattice $\mathbb{Z}^3\Delta$ (i.e., a coordinate lattice with unit size Δ) which have non-empty intersection with bounded set $X \subset \mathbb{R}^3$. Also for the bounded set $X \subset \mathbb{R}^2$, denote by $\mu(X)$ the (Lebesgue) measure of the set X. Further, denote by $N_X(\Delta)$ the number of squares from corresponding $\mathbb{Z}^2\Delta$ lattice in a plane that has non-empty intersection with $X \subset \mathbb{R}^2$.

The following definition of the box-counting dimension $\dim_b(X)$ of the bounded set $X \subset \mathbb{R}^3$ is well-known (see for example [22]):

$$\dim_b(X) = \lim_{\Delta\to 0} -\frac{\log N_X(\Delta)}{\log \Delta}. \tag{4}$$

It is also well-known (see for example [22]) that the box-counting dimensions of the surface $\mathcal{S}$ is equal to $\dim_b(\mathcal{S}) = 2$. This means that for each $\epsilon > 0$, there is $\Delta_\epsilon > 0$ such that $N_\mathcal{S}(\Delta)\Delta^2 \in (\Delta^\epsilon, \Delta^{-\epsilon})$ holds for each $\Delta < \Delta_\epsilon$. However, it does not automatically imply that $N_\mathcal{S}(\Delta)\Delta^2$ converges to some constant C (when $\Delta \to 0$). Even more, it does not even imply that $N_\mathcal{S}(\Delta)\Delta^2$ is bounded either from the top or from the bottom. In the rest of this Section we show that $N_\mathcal{S}(\Delta)\Delta^2$ converges (when $\Delta \to 0$) and we find its limit value.

4.2. Preliminary results

Assume that $\mathcal{S}$ does not pass through any node of lattice $\mathbb{Z}^3\Delta$. Without loss of generality, assume that $\mathcal{S}_{xy}$ lies in the first quadrant of the xy coordinate plane. Denote by $B_{kl} = [k\Delta, (k+1)\Delta] \times [l\Delta, (l+1)\Delta]$ and

$$\bar{F}_{k,l} = \left\lceil \max_{(x,y)\in\mathcal{S}_{xy}\cap B_{kl}} f(x,y)/\Delta \right\rceil, \quad F_{k,l} = \left\lfloor \min_{(x,y)\in\mathcal{S}_{xy}\cap B_{kl}} f(x,y)/\Delta \right\rfloor$$

for every $k, l \in \mathbb{N}_0$ such that B_{kl} have non-empty intersection with $\mathcal{S}_{xy}$. The following propositions directly follow from continuity of f.

Proposition 4.1. *The number of coordinate boxes with the base B_{kl} having non-empty intersection with $\mathcal{S}$ is equal to $\bar{F}_{k,l} - F_{k,l}$. Hence,*

$$N_{\mathcal{S}}(\Delta) = \sum_{B_{kl}\cap\mathcal{S}_{xy}\neq\emptyset} (\bar{F}_{k,l} - F_{k,l}). \tag{5}$$

Proposition 4.2. *If $X \subset \mathbb{R}^2$ is compact then*

$$\lim_{\Delta\to 0} N_X(\Delta)\Delta^2 = \mu(X).$$

Proposition 4.3. *If $\gamma \subset \mathbb{R}^3$ is any set with box-counting dimension less than 2, then $N_\gamma(\Delta)\Delta^2 \to 0$ when $\Delta \to 0$.*

Proof. Assume that $d = \dim_b(\gamma)$. According to (4), we get $N_\gamma(\Delta) \leqslant \Delta^{-d-\epsilon}$ for some $\epsilon < 2 - d$ and $\Delta < \Delta_\epsilon$. Hence

$$N_\gamma(\Delta)\Delta^2 \leqslant \Delta^{2-d-\epsilon} \to 0, \qquad \Delta \to 0.$$

This completes the proof. □

Corollary 4.1. *If $\gamma \subset \mathbb{R}^3$ is a finite union of $\mathcal{C}^{(1)}$ curves, then $N_\gamma(\Delta)\Delta^2 \to 0$ when $\Delta \to 0$.*

Proof. It is well-known (see for example [22]) that $\dim_b(\gamma) = 1$. Now the statement of the corollary follows directly from the previous proposition. □

Denote by $\delta\mathcal{S}$ the boundary of a surface $\mathcal{S}$ and by δX the boundary of a compact set $X \subset \mathbb{R}^2$. In what follows, we always assume that the boundary of every surface is a piecewise $\mathcal{C}^{(1)}$ curve.

Proposition 4.4. *If $\mathcal{S} = \mathcal{S}^1 \cup \mathcal{S}^2 \cup \cdots \cup \mathcal{S}^v$, where $\mathcal{S}^i$ and $\mathcal{S}^j$ may have only boundary points in common (in other words $\mathcal{S}^i \cap \mathcal{S}^j \subset \delta\mathcal{S}^i \cup \delta\mathcal{S}^j$) then*

$$0 \leqslant \sum_{i=1}^{v} N_{\mathcal{S}^i}(\Delta) - N_{\mathcal{S}}(\Delta) \leqslant (v-1)N_\gamma(\Delta)$$

where $\gamma = \cup_{i=1}^{v}\delta\mathcal{S}^i$. If $N_{\mathcal{S}^i}(\Delta)\Delta^2 \to L_i$ when $\Delta \to 0$ for every $i = 1, 2, \ldots, v$, then $N_{\mathcal{S}}(\Delta)\Delta^2 \to \sum_{i=1}^{v} L_i$ when $\Delta \to 0$.

Proof. Denote by $s = \sum_{i=1}^{v} N_{\mathcal{S}^i}(\Delta)$. Assume that a coordinate box B intersects $\mathcal{S}$ but not γ. Then, there is exactly one i such that B intersects $\mathcal{S}_i$. Those boxes are counted once in s. On the other hand, if B intersects γ, it might intersect more than one surface $\mathcal{S}_i$. Those boxes are counted at most v times in s. Therefore, the difference

$$\sum_{i=1}^{v} N_{\mathcal{S}^i}(\Delta) - N_{\mathcal{S}}(\Delta)$$

gives the number of all additional counts of boxes, which are at most $(v-1)N_\gamma(\Delta)$.

The second part follows from the fact that $\delta\mathcal{S}_i$ is a piecewise $\mathcal{C}^{(1)}$ curve, implying that γ is finite union of such curves and $N_\gamma(\Delta)\Delta^2 \to 0$ according to Corollary 4.1. □

Denote by $N_{\mathcal{S}}^{int}(\Delta)$ the number of boxes B which intersect $\mathcal{S}$ but not $\delta\mathcal{S}$. In the same sense, denote by $N_{\mathcal{S}}^{\delta}(\Delta) = N_{\delta\mathcal{S}}(\Delta)$ the number of boxes having non-empty intersection with $\delta\mathcal{S}$. It is obvious that $N_{\mathcal{S}}(\Delta) = N_{\mathcal{S}}^{int}(\Delta) + N_{\mathcal{S}}^{\delta}(\Delta)$. Moreover, if B intersects $\mathcal{S}$ but not $\delta\mathcal{S}$, then its projection B_{kl} on the xy plane intersects $\mathcal{S}_{xy}$ but not $\delta\mathcal{S}_{xy}$. Therefore $B_{kl} \subset \iint \mathcal{S}_{xy}$ and from Proposition 4.1 it holds that

$$N_{\mathcal{S}}^{int}(\Delta) = \sum_{B_{kl}\subset \mathrm{int}\mathcal{S}_{xy}} \left(\bar{F}_{k,l} - F_{k,l}\right). \tag{6}$$

Lemma 4.1. *Assume that $\mathcal{S}_{xy}$ is compact with non-empty interior and denote by*

$$M_{\mathcal{S}} = \max_{(x,y)\in\mathcal{S}_{xy}} \frac{\partial f}{\partial x}(x,y) + \max_{(x,y)\in\mathcal{S}_{xy}} \frac{\partial f}{\partial y}(x,y) + 2. \qquad (7)$$

Then

$$N_{\mathcal{S}}^{int}(\Delta) \leqslant M_{\mathcal{S}} \cdot N_{\mathcal{S}_{xy}}(\Delta).$$

Proof. Assume that $B_{kl} \subset \mathcal{S}_{xy}$. Since f is continuous and B_{kl} is compact, there exist points $(x_0,y_0),(x_1,y_1) \in B_{kl} \cap \mathcal{S}_{xy}$ where $f(x,y)$ attains its minimum and maximum values, respectively, i.e., $F_{k,l} = \lfloor f(x_0,y_0)/\Delta \rfloor$ and $\bar{F}_{k,l} = \lceil f(x_1,y_1)/\Delta \rceil$. According to the Lagrange theorem, there exists (x',y') on the line connecting (x_0,y_0) and (x_1,y_1), such that

$$\begin{aligned} \bar{F}_{k,l} - F_{k,l} &\leqslant \tfrac{f(x_1,y_1)-f(x_0,y_0)}{\Delta} + 2 \\ &\leqslant [\tfrac{\partial f}{\partial x}(x',y')\tfrac{x_1-x_0}{\Delta} + \tfrac{\partial f}{\partial y}(x',y')\tfrac{y_1-y_0}{\Delta}] + 2 \\ &\leqslant \tfrac{\partial f}{\partial x}(x',y') + \tfrac{\partial f}{\partial y}(x',y') + 2 \leqslant M_{\mathcal{S}}. \end{aligned}$$

The number of boxes $B_{kl} \subset \mathcal{S}_{xy}$ is less than or equal to $N_{\mathcal{S}_{xy}}(\Delta)$ and hence it is valid:

$$N_{\mathcal{S}}^{int}(\Delta) \leqslant M_{\mathcal{S}} N_{\mathcal{S}_{xy}}(\Delta).$$

This completes the proof. □

4.3. Main result

Assume now that $\mathcal{S}$ can be represented in the same way as in (3), but taking $\mathcal{S}_{xz}$ and $\mathcal{S}_{yz}$ respectively as the domain of the function f. In other words, assume that

$$\mathcal{S} = \{(x, f_{xz}(x,z), z) | (x,z) \in \mathcal{S}_{xz}\} = \{(f_{yz}(y,z), y, z) | (y,z) \in \mathcal{S}_{yz}\}.$$

It can be easily seen that $f(\bar{x},\cdot)$ and $f(\cdot,\bar{y})$ are bijections. Indeed, if $z = f(\bar{x},y_0) = f(\bar{x},y_1)$, for some $(\bar{x},y_0),(\bar{x},y_1) \in \mathcal{S}_{xy}$, then $(\bar{x},y_0,\bar{z}) \in \mathcal{S}$ and $(\bar{x},y_1,\bar{z}) \in \mathcal{S}$ which implies that $y_0 = y_1 = f_{xz}(\bar{x},\bar{z})$. Assume that $\partial f/\partial x(x',y') = 0$ for some $(x',y') \in \mathrm{int}\mathcal{S}_{xy}$. Consider the function $f(\cdot,y')$ in the neighborhood of (x',y'). It has a local minimum in x' which means that it is not a bijection. Therefore, $\partial f/\partial x \neq 0$ and hence it does not change its sign on $\mathcal{S}_{xy}$. The same holds for $\partial f/\partial y$. Without loosing generality, we may assume that both partial derivatives are positive on $\mathcal{S}_{xy}$.

In what follows, we show the proof of the following theorem.

Theorem 4.1. *The following is valid*

$$\lim_{\Delta\to 0} N_{\mathcal{S}}(\Delta)\Delta^2 = P(\mathcal{S}) = \mu(\mathcal{S}_{xy}) + \mu(\mathcal{S}_{yz}) + \mu(S_{xz}) \qquad (8)$$

where the limit is taken over those values Δ such that $\mathcal{S}$ do not contain any node of the lattice $\mathbb{Z}^3\Delta$.

First we prove the theorem for rectangular $\mathcal{S}_{xy}$.

Lemma 4.2. *Assume that $\mathcal{S}_{xy}$ is rectangle $[x_{min}, x_{max}] \times [y_{min}, y_{max}]$. Then (8) is valid.*

Proof. Without loss of generality, assume that $x_{min} \in [0,\Delta)$. If the latter is not true, then translate the surface by the vector $(\lfloor x_{min}/\Delta \rfloor \Delta, 0, 0)$. In the same way, assume that $y_{min} \in [0,\Delta)$. Let $m = \lfloor x_{max}/\Delta \rfloor$ and $n = \lfloor y_{max}/\Delta \rfloor$. Furthermore, define

$$x_k = \begin{cases} x_{min}, & k = 0 \\ k\Delta, & k = 1,2\ldots,m \\ x_{max}, & k = m+1. \end{cases}$$

and analogously y_l for $l = 0,1,\ldots,n+1$. According to Proposition 4.1, we have

$$N_{\mathcal{S}}(\Delta) = \sum_{k=0}^{m}\sum_{l=0}^{n}(\bar{F}_{k,l} - F_{k,l}). \qquad (9)$$

Note that $B_{kl} \subset \mathcal{S}_{xy}$ for $k = 1,2,\ldots,m-1$ and $l = 1,2,\ldots,n-1$. Since $f(x,y)$ is monotonically increasing function of both x and y, we conclude that

$$\begin{aligned} F_{k,l} &= \lfloor f(x_k,y_l)/\Delta \rfloor \\ \bar{F}_{k,l} &= \lceil f(x_{k+1},y_{l+1})/\Delta \rceil = F_{k+1,l+1} + 1 \\ k &= 1,\ldots,m-1, \\ l &= 1,\ldots,n-1. \end{aligned}$$

Replacing this in (9) yields

$$N_{\mathcal{S}}(\Delta) = mn + \sum_{k=0}^{m} (\bar{F}_{k,n} - F_{k,0}) + \sum_{l=0}^{n} (\bar{F}_{m,l} - F_{0,l}) - (\bar{F}_{m,n} - F_{0,0}). \tag{10}$$

Now consider $\mathcal{S}_{xz}$. Due to the continuity and monotonicity of f, it can be written in the form

$$\mathcal{S}_{xz} = \{(x,z) | x \in [x_{min}, x_{max}],\ z \in [f(x, y_{min}), f(x, y_{max})]\}.$$

Thus, it is evident that the number of boxes of $\mathbb{Z}^2\Delta$ having non-empty intersection with $\mathcal{S}_{xz} \cap ([x_k, x_{k+1}] \times \mathbb{R})$ is equal to

$$\bar{F}_{k,n} - F_{k,0} = \lceil f(x_{k+1}, y_{max})/\Delta \rceil - \lfloor f(x_k, y_{max})/\Delta \rfloor.$$

Therefore, the first sum in (10) is equal to $N_{S_{xz}}(\Delta)$. The same way, the second sum is $N_{S_{yz}}(\Delta)$. According to these, we now have

$$N_{\mathcal{S}}(\Delta)\Delta^2 = mn\Delta^2 + N_{S_{xz}}(\Delta)\Delta^2 + N_{S_{yz}}(\Delta)\Delta^2 - (\bar{F}_{m,n} - F_{0,0})\Delta^2. \tag{11}$$

Since $|x_{min}| < \Delta$ (by assumption from the beginning of the proof), we get

$$|x_{max} - x_{min} - m\Delta| \leqslant |x_{max} - m\Delta| + \Delta \leqslant 2\Delta$$

and similarly $|y_{max} - y_{min} - n\Delta| \leqslant 2\Delta$. Hence, the limit of the first term in (11) is $\mu(S_{xy}) = (x_{max} - x_{min})(y_{max} - y_{min})$, when $\Delta \to 0$. Proposition 4.2 implies that the second and third term in (11) tend to $\mu(\mathcal{S}_{xz})$ and $\mu(\mathcal{S}_{yz})$ respectively. Finally, the forth term can be bounded as

$$(\bar{F}_{m,n} - F_{0,0})\Delta^2 \leqslant \left[\frac{f(x_{max}, y_{max})}{\Delta} - \frac{f(x_{min}, y_{min})}{\Delta} + 2\right]\Delta^2$$

and hence tends to 0. This completes the proof of the Lemma 4.2. □

Proof (*Proof of the main theorem*). Since $\mathcal{S}_{xy}$ is compact, it can be approximated by the union of rectangles $R_i \subseteq \mathcal{S}_{xy}, i = 1, 2, \ldots, v$ having only boundary points in common, such that

$$\mu(\bar{\mathcal{S}}_{xy}) < \frac{\epsilon}{12M_{\mathcal{S}}}, \quad \bar{\mathcal{S}}_{xy} = \mathcal{S}_{xy} \setminus R, \quad R = \cup_{i=1}^{v} R_i$$

and $P(\mathcal{S}) - P(\mathcal{S}_R) < \epsilon/3$, where $\epsilon > 0$ is arbitrary and

$$\mathcal{S}_R = \{(x, y, f(x, y)) | (x, y) \in R\}$$

is a surface induced by the union of the rectangles R. The same way, define $\mathcal{S}_{R_i}$ and $\mathcal{S}_\gamma$ where $\gamma = \cup_{i=1}^{v} \delta S_{R_i} \cup \delta\mathcal{S}$. Furthermore, let $\bar{\mathcal{S}} = \mathcal{S} \setminus \mathcal{S}_R$. Note that $\delta\bar{\mathcal{S}} = \delta S_R \cup \delta\mathcal{S} \subseteq \gamma$. According to Lemma 4.2 and Proposition 4.4, there exist $\Delta_1 > 0$ such that

$$\left| N_{\mathcal{S}_R}(\Delta)\Delta^2 - P(\mathcal{S}_R) \right| \leqslant \frac{\epsilon}{3}$$

for all $\Delta \leqslant \Delta_1$. Furthermore, according to Proposition 4.4 we have

$$|N_{\mathcal{S}}(\Delta)\Delta^2 - N_{\mathcal{S}_R}(\Delta)\Delta^2| \leqslant N_{\bar{\mathcal{S}}}(\Delta)\Delta^2 + vN_\gamma(\Delta)\Delta^2 \leqslant N_{\bar{\mathcal{S}}}^{int}(\Delta)\Delta^2 + (v+1)N_\gamma(\Delta)\Delta^2.$$

The last inequality holds since $\delta\bar{\mathcal{S}} \subseteq \gamma$ and hence $N_{\bar{\mathcal{S}}}^{\delta}(\Delta) = N_{\delta\bar{\mathcal{S}}}(\Delta) \leqslant N_\gamma(\Delta)$. The first term can be bounded (Lemma 4.1) by:

$$N_{\bar{\mathcal{S}}}^{int}(\Delta)\Delta^2 \leqslant M_{\bar{\mathcal{S}}} \cdot N_{\bar{\mathcal{S}}_{xy}}(\Delta)\Delta^2 \leqslant M_{\mathcal{S}} \cdot N_{\bar{\mathcal{S}}_{xy}}(\Delta)\Delta^2.$$

Here we used that $M_{\bar{\mathcal{S}}} \leqslant M_{\mathcal{S}}$ since the maximum is taken over the larger set (see (7)). According to Proposition 4.2, we can choose $\Delta_2 > 0$ such that $|N_{\bar{\mathcal{S}}_{xy}}(\Delta)\Delta^2 - \mu(\bar{\mathcal{S}}_{xy})| \leqslant \epsilon/(12M_{\mathcal{S}})$ for all $\Delta \leqslant \Delta_2$. Then

$$|N_{\bar{\mathcal{S}}_{xy}}(\Delta)\Delta^2| \leqslant \frac{\epsilon}{12M_{\mathcal{S}}} + \mu(\bar{\mathcal{S}}_{xy}) \leqslant \frac{\epsilon}{6M_{\mathcal{S}}}$$

and

$$N_{\bar{\mathcal{S}}}^{int}(\Delta)\Delta^2 \leqslant M_{\bar{\mathcal{S}}} \frac{\epsilon}{6M_{\mathcal{S}}} \leqslant \frac{\epsilon}{6}.$$

Corollary 4.1 yields that there exists $\Delta_3 > 0$ such that $N_\gamma(\Delta)\Delta^2 < \epsilon/(6(v+1))$ for all $\Delta \leqslant \Delta_3$. Putting everything together, we get

$$|N_{\mathcal{S}}(\Delta)\Delta^2 - N_{\mathcal{S}_R}(\Delta)\Delta^2| \leqslant \frac{\epsilon}{3}.$$

Finally

$$|N_{\mathcal{S}}(\Delta)\Delta^2 - P(\mathcal{S})| \leqslant |N_{\mathcal{S}}(\Delta)\Delta^2 - N_{\mathcal{S}_R}(\Delta)\Delta^2| + |N_{\mathcal{S}_R}(\Delta)\Delta^2 - P(\mathcal{S}_R)| + |P(\mathcal{S}_R) - P(\mathcal{S})| \leqslant \epsilon$$

for every $\Delta < \min\{\Delta_1, \Delta_2, \Delta_3\}$. This completes the proof of the theorem. □

4.4. Extensions on arbitrary (piecewise) $\mathcal{C}^{(1)}$ surfaces

Theorem 4.1 implies that $N_{\mathcal{S}}(\Delta)\Delta^2$ tends to $P(\mathcal{S})$ when $\Delta \to 0$, if $\mathcal{S}$ is a graph surface of the $\mathcal{C}^{(1)}$ function f defined on the compact $\mathcal{S}_{xy}$. Moreover, assumption is that $\mathcal{S}$ can be also represented as the graph surface on $\mathcal{S}_{yz}$ and $\mathcal{S}_{xz}$.

Note that any $\mathcal{C}^{(1)}$ surface can be divided on finitely many graph surfaces. Also, each graph $\mathcal{C}^{(1)}$ surface can be divided on finitely many surfaces that can be represented as graph surfaces on all three projections.

In that sense, every $\mathcal{C}^{(1)}$ surface $\mathcal{S}$ can be divided on finitely many $\mathcal{C}^{(1)}$ surfaces $\mathcal{S}^i, i = 1, 2, \ldots, m$ satisfying the conditions assumed in the previous section. According to Proposition 4.4 and Theorem 4.1, we conclude that

$$\lim_{\Delta\to 0} N_{\mathcal{S}}(\Delta)\Delta^2 = \sum_{i=1}^{m} P(\mathcal{S}^i).$$

Therefore, the following Corollary holds, which is equivalent to Theorem 3.1.

Corollary 4.2. *Let $\mathcal{S}$ be a union of a finite number of $\mathcal{C}^{(1)}$ surfaces. Then,*

$$\lim_{\Delta\to 0} N_{\mathcal{S}}(\Delta)\Delta^2 = C$$

where C is a constant.

5. Discussion and conclusion

In this paper, we considered the problem of indexing cells on a uniform grid intersecting with a union of a finite number of $\mathcal{C}^{(1)}$ surfaces. As a main result, we prove that the problem has quadratic asymptotic complexity in the reciprocal linear size of a grid cell. Also, we demonstrated that a practical recursive partitioning algorithm [11] that indexes the grid cells intersecting with the surfaces achieves the problem complexity bound and therefore is asymptotically optimal. We believe this opens the venue for further application of the algorithm in multi-scale simulation.

Note that in [11], a statistical analysis of the algorithm complexity was performed. There, execution time of multiple runs of the algorithm implementation was regressed as a function of a power of a reciprocal linear size of a grid cell. Using the t-test, the hypothesis that the power coefficient of the regression model is 2 could not be rejected with significance $\alpha = 0.05$ (see e.g., [23] for details on regression models estimation and inference). These results are consistent with the theoretical considerations presented in this paper.

Work continues on generalization of the main result when the indexed surface has a box-counting dimension different from 2.

Acknowledgement

This project was supported by a grant from the National Institute of General Medical Sciences (P20 GM103446) from the National Institutes of Health. The work was partially supported by the US Department of Defense Breast Cancer Research Program (HBCU Partnership Training Award #BC083639), the US National Institutes of Health (R01 grant #CA154444), the US National Science Foundation (CREST grant #HRD-1242067), and the US Department of Defense/Department of Army (Awards #45395-MA-ISP, #54412-CI-ISP, #W911NF-11–2-0046). M.D. Petković was supported by research project 174013 of the Serbian Ministry of Science and DoD/DoA (Award 45395-MA-ISP).

References

[1] D. Meagher, Geometric modeling using octree encoding, Comput. Graphics Image Process. 19 (1982) 129–147.
[2] H. Samet, The quadtree and related hierarchical data structures, ACM Comput. Surv. (CSUR) 16 (2) (1984) 187–260.
[3] H. Samet, A. Kochut, Octree approximation and compression methods, in: Proceedings First International Symposium on 3D Data Processing Visualization and Transmission, 2002, pp. 460–469.
[4] J. Wilhelms, A. Van Gelder, Octrees for faster isosurface generation, IEEE Trans. Med. Imaging 19 (2000) 739–758.
[5] W. Song, S. Hua, Z. Ou, H. An, Octree based representation and volume rendering of three-dimensional medical data sets, in: Proceedings International Conference on BioMedical Engineering and Informatics, BMEI, 2008, pp. 316–320.
[6] A. Badal, I. Kyprianou, A. Badano, K.J. Myers, J. Sempau, Monte Carlo package for simulating radiographic images of realistic anthropomorphic phantoms described by triangle meshes, Medical Imaging 2007, Proc. SPIE 6510 (2007) 65100Z.
[7] W.-T. Wong, F.Y. Shih, T.-F. Su, Thinning algorithms based on quadtree and octree representations, Inf. Sci. 176 (2006) 1379–1394.
[8] H. Lee, M. Desbrun, P. Schöder, Progressive encoding of complex isosurfaces, in: Proceedings ACM SIGGRAPH 2003 Conference, 2003, pp. 471–476.
[9] K. Zhou, M. Gong, X.H. Baining, Data-parallel octrees for surface reconstruction, IEEE Trans. Visual. Comput. Graphics 17 (5) (2011) 669–681.
[10] J.H. Chui, D.D. Pokrajac, A.D.A. Maidment, P.R. Bakic, Towards breast anatomy simulation using GPUs, in: Proceedings 11th International Workshop on Breast Imaging (IWDM 2012), Lecture Notes in Computer Science 7361, 2012, pp. 506–513.
[11] D.D. Pokrajac, A.D.A. Maidment, P.R. Bakic, Optimized generation of high resolution breast anthropomorphic software phantoms, Med. Phys. 39 (2012) 2290–2302.
[12] J. Chui, D. Pokrajac, A.D. Maidment, P. Bakic, Roadmap for Efficient Parallelization of Breast Anatomy Simulation, Medical Imaging 2012, Proc. SPIE 8313, 2012, 83134T.
[13] F. Chen, D. Pokrajac, F. Liu, A.D. Maidment, P. Bakic, Partial volume effect simulation in software breast phantoms, in: cal Imaging 2012, Proc. SPIE 8313, 2012, 83134U.

[14] F. Chen, D. Pokrajac, X. Shi, F. Liu, A.D. Maidment, P. Bakic, Simulation of three materials partial volume averaging in a software breast phantom, in: Proc. 11th International Workshop on Breast Imaging (IWDM), Lecture Notes in Computer Science 7361, 2012, pp. 151-158.
[15] J. Chui, R. Zeng, D. Pokrajac, S. Park, K.J. Myers, A.D.A. Maidment, P.R. Bakic, Two methods for simulation of dense tissue distribution in software breast phantoms, in: Medical Imaging 2013, Proc. SPIE 8668, 2013, 86680M.
[16] C.K. Abbey, P.R. Bakic, D.D. Pokrajac, A.D.A. Maidment, M.P. Eckstein, J.M. Boone, Non-gaussian statistical properties of virtual breast phantoms, in: Medical Imaging 2014: Image Perception, Observer Performance, and Technology Assessment, Proc. SPIE 9037, 2014, 90370G.
[17] P.R. Bakic, D.D. Pokrajac, R. DeCaro, A.D.A. Maidment, Realistic Simulation of Breast Tissue Microstructure in Software Anthropomorphic Phantoms. in: Proceedings 12th International Workshop on Breast Imaging (IWDM), Lecture Notes in Computer Science 8539, pp. 348–355.
[18] A.D.A. Maidment, Virtual clinical trials for the assessment of novel breast screening modalities, in: Proceedings 12th International Workshop on Breast Imaging (IWDM), Lecture Notes in Computer Science 8539, 2014, pp. 1–8.
[19] P. Liu, G.-F. Chen, Porous Materials: Processing and Applications, Butterworth-Heinemann, Oxford, UK, 2014.
[20] L. Alberti, G. Comte, B. Mourrain, Meshing implicit algebraic surfaces: the smooth case, in: Proceedings Conference on Mathematical Methods for Curves and Surfaces, 2005, pp. 11–26.
[21] E.F. Moore, The shortest path through a maze, in: Proceedings of the International Symposium on the Theory of Switching, 1959, pp. 285–292.
[22] K. Falconer, Fractal geometry – Mathematical Foundations and Applications, second edition., Wiley, 2003.
[23] J.L. Devore, Probability and Statistics for Engineering and the Sciences, Brooks/Cole, Belmont, CA, 2008.